LIMNOLOGY
and
OCEANOGRAPHY

ASLO

Limnol. Oceanogr. 61, 2016, S238–S252

doi: 10.1002/lno.10298

Spatio-temporal variability of methane (CH_4) concentrations and diffusive fluxes from a tropical coastal embayment surrounded by a large urban area (Guanabara Bay, Rio de Janeiro, Brazil)

Luiz C. Cotovicz Jr.,*[1,2] Bastiaan A. Knoppers,[1] Nilva Brandini,[1] Dominique Poirier,[2] Suzan J. Costa Santos,[1] Gwenaël Abril[1,2]

[1]Programa de Geoquímica, Universidade Federal Fluminense, Niterói, Rio de Janeiro, Brazil
[2]Laboratoire Environnements et Paléoenvironnements Océaniques et Continentaux (EPOC), CNRS, Université de Bordeaux, Pessac Cedex France

Abstract

The increasing concentrations of methane (CH_4) in the atmosphere stress the importance of monitoring and quantifying the fluxes from coastal environments. In nine sampling campaigns between 2013 and 2014, we measured the spatial CH_4 concentrations, identified major sources and calculated the fluxes at the air-water interface in an eutrophic tropical embayment, Guanabara Bay, Rio de Janeiro, Brazil. The bay presented high spatial variability of CH_4 concentrations, without a significant trend with salinity, but observed the influence of the urban areas at its watershed. Although the more polluted sector of the bay accounts for about 10% of the sampled surface area, it contributed to one half of the bay's total CH_4 emissions. In most cases, high CH_4 concentrations seemed be sustained by allochtonous sources such as the sewage network and polluted rivers, especially under high accumulated precipitation conditions. In the most stratified area, at the inner and centre of the Bay, CH_4 concentrations were not significantly higher in bottom hypoxic waters than in surface waters, suggesting that CH_4 diffusion from these sediments was modest, due to the prevalence of sulphate reduction over methanogenesis. Our calculated annual air-sea fluxes (565–980 μmol m^{-2} d^{-1}) are well above those of most estuaries worldwide, showing that urban pollution can be an important source of CH_4 to the coastal waters and even more significant than the presence of organic-rich environments, like salt marshes and mangroves. Comparing the greenhouse gas emissions in terms of CO_2-equivalent, CH_4 emissions reduced the net CO_2 sink in Guanabara Bay by 16%.

Since the beginning of the industrial era, emissions of greenhouse gases due to human activities have led to a marked increase in their atmospheric concentrations (IPCC 2013). Methane (CH_4) is an important and effective greenhouse gas with a molecule-for-molecule basis about 28 times more efficient in trapping radiation than carbon dioxide (CO_2) as established for a 100 yr period (IPCC 2013). The concentration of CH_4 in the atmosphere has increased by a factor of 2.5 since pre-industrial times, from 0.7 μatm in 1750 to 1.8 μatm in 2011 (present emissions are 553 Tg yr^{-1}), and exceeded the pre-industrial levels by about 150%, with some projections indicating a further doubling by 2100 (IPCC 2013).

Despite the small surface area compared with the open ocean, the coastal ocean contributes to about 75% of global oceanic methane emissions (Bange 2006; Reeburgh 2007). This reflects larger inputs and sedimentation rates of reactive organic matter arising from continental sources (Bousquet et al. 2006; EPA 2010). The spatial distribution of CH_4 concentrations in some estuaries appears to be partly controlled by inputs from high-CH_4 concentrations in river waters, which mix with low-CH_4 concentrations in seawaters, converging to the general spatial profile of high-CH4 waters in the upper sections and low salinity areas of estuaries (de Angelis and Lilley 1987; Upstill-Goddard et al. 2000; Middelburg et al. 2002). Up to 90% of the riverine CH_4 input to estuaries is lost to the atmosphere during its transport, with only a small fraction being oxidized in the water column (Upstill-Goddard et al. 2000; Abril and Iversen 2002). In

*Correspondence: lccjunior@id.uff.br

Additional Supporting Information may be found in the online version of this article.

Special Issue: Methane Emissions from Oceans, Wetlands, and Freshwater Habitats: New Perspectives and Feedbacks on Climate.
Edited by: Kimberly Wickland and Leila Hamdan.

coastal areas, the ecosystem and habitat heterogeneity ensures several transport pathways of CH_4 to the atmosphere, including water-air (and soil-water) diffusion, ebullition through the water column, ebullition at low tide in intertidal areas, transport through plants in tidal wetlands, and tidal pumping, i.e., transport of dissolved CH_4 from the intertidal areas to the channels with ebb tide (de Angelis and Scranton 1993; Sansone et al. 1999; Abril and Iversen 2002; Middleburg et al. 2002; Borges and Abril 2011). In estuaries, the balance between methanogenesis and methanotrophy is driven by microbial and physical processes that are highly variable depending on the inputs of reactive organic matter to the sediments, availability of electron acceptors, hydrodynamics, hydrostatic pressure, salinity and temperature (Martens et al. 1998; Borges and Abril 2011). In general, methane production is greater in freshwater areas because the high sulphate availability in marine waters inhibits methane production, which starts to occur deeper in the sediments, when sulphate becomes depleted (Martens and Berner 1974). High methanogenesis in marine sediments was documented in estuaries that present extremely high sedimentation rates of reactive organic matter that can lead to a rapid sulphate depletion in the top layers of the sediments (Martens et al. 1998). The competition between sulphate reduction and methanogenesis processes can also explain the general seaward decrease in CH_4 concentrations and fluxes (Borges and Abril 2011).

The high spatial and temporal heterogeneity in the methanogenesis, methanotrophy and transport patterns make it difficult to estimate precise estuarine global emissions of CH_4 (Bange 2006; Borges and Abril 2011). A recent analysis of CH_4 emission patterns in boreal, temperate, and tropical estuarine systems, revealed a high spatial variability depending on their typology, and their respective organic carbon sedimentation rates and salinities (Borges and Abril 2011). The uncertainties in the fluxes at the coastal zone are attributed to sparse data collection, poor habitat/typology coverage, lack of tropical and southern latitude sampling, and the absence of seasonal, annual or interannual temporal studies. Most of the studies were conducted in river-dominated and temperate estuaries and little is known about the CH_4 emissions in marine-dominated systems such as lagoons and coastal bays. Concerning diffusion only, the CH_4 water-air flux varies from 0.04 ± 0.17 mmol C m^{-2} d^{-1} for coastal plumes and open waters to 1.85 ± 0.99 mmol C m^{-2} d^{-1} for fjords and coastal lagoons, with intermediate values for low salinity zones, marsh and mangrove creeks (Borges and Abril 2011). The very high standard deviations of these values represent large uncertainties in the estimated fluxes.

Another point recently discussed is the perturbation of the coastal CH_4 balance driven by organic pollution and eutrophication (Bange 2006; Nirmal Rajkumar et al. 2008; Allen et al. 2010; Castro-Morales et al. 2014; Burgos et al. 2015). Indeed, extremely high emissions of CH_4 were found in some highly polluted systems especially closer to the discharge of wastewater and at localities under strong anthropogenic influence (Nirmal Rajkumar et al. 2008; Burgos et al. 2015). The dissolved CH_4 concentrations and emissions can span several orders of magnitude both spatially and temporally in estuaries subject to effluent contamination and eutrophication (Nirmal Rajkumar et al. 2008). Also, studies comparing pristine and perturbed systems showed lower CH_4 waters in pristine environments (Kristensen et al. 2008; Allen et al. 2010). An increase in CH_4 emissions may be expected for developing countries (most located in tropical regions) taking account the current low coverage of wastewater treatment plans in these countries and the fast rates of population growth, particularly in coastal regions. Thus, the monitoring and quantification of the CH_4 concentrations and fluxes in polluted and eutrophic estuarine systems can become a significant issue in the coastal carbon cycle.

The aims of this study are to document spatial and temporal variability in CH_4 concentrations and to calculate diffusive CH_4 fluxes in a highly polluted and eutrophic tropical marine embayment, Guanabara Bay, Rio de Janeiro State, Brazil. The objectives include identifying the sectors of CH_4 emissions in the bay, discuss the origin of CH_4 concentrations and quantify the diffusive fluxes at the air-water interface at the local scale of the sampled area. We describe how anthropogenic activities affect the CH_4 emissions in densely populated coastal areas and more precisely in tropical marine-dominated estuaries for which there is still paucity of information. Further, we compare the CH_4 concentrations in Guanabara Bay with those from other estuarine types in different climatic regions.

Material and methods

Study site

Guanabara Bay (22°41–22°58 S and 43°02–43°18 W) is located at the SE-Brazil coast, and is surrounded by the metropolitan area of Rio de Janeiro city, the second most populous region of Brazil (Fig. 1). The bay has a surface area of 384 km^2, a mean depth of about 5.7 m, and a water volume of 1870×10^6 m^3. It is characterized by a microtidal regime (tidal amplitude of 0.7 m on average and 1.3 m at spring tides), and is a partially mixed estuary (Kjerfve et al. 1997) that can become stratified in summertime due to concomitant effects of sunlight and freshwater discharge (Bérgamo 2006; Cotovicz et al. 2015). Salinity varies between 25 and 34, with exceptions of the outlet of small rivers where the salinity is lower. The residence time for renewal of 50% of the total water volume is 11.4 days (Kjerfve et al. 1997). At the bay's mouth, maximum water velocities vary between 0.8 m s^{-1} and 1.5 m s^{-1}, whereas at the most confined upper northern sectors the maximum current velocities are 0.3 m s^{-1}, and residence times of the water are longer (Kjerfve et al. 1997). Guanabara Bay is located in the

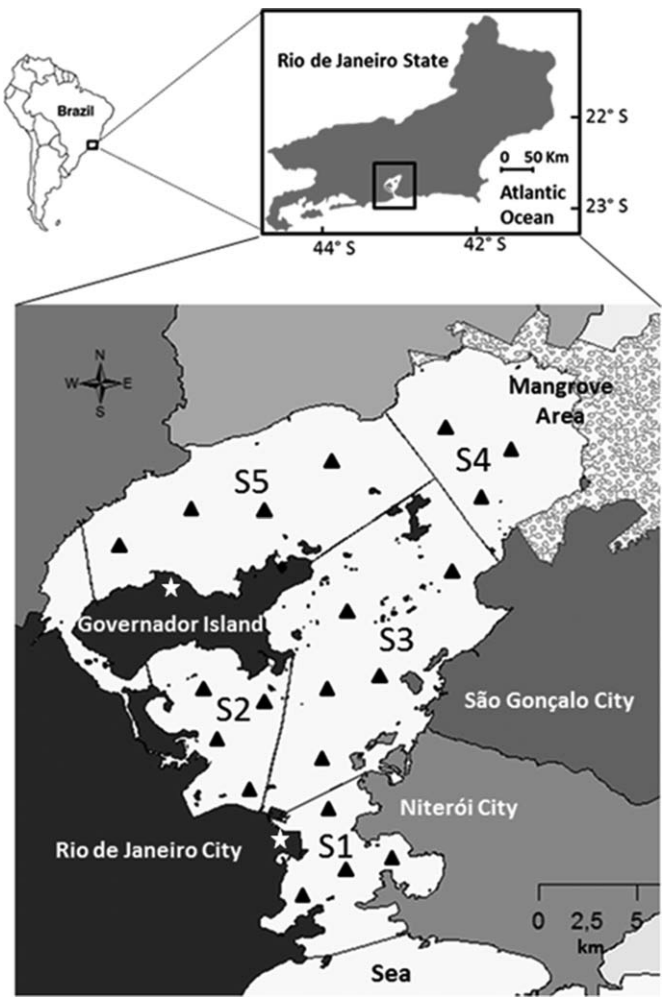

Fig. 1. Location of the Guanabara Bay, Rio de Janeiro, Brazil. The Bay was divided into five sectors to analyse spatial heterogeneity. The black triangles represent the sampling stations. The two white stars represent the locations of the airports with the meteorological stations. The different colour tonalities represents the demographic occupation around the bay, with the most dark colour representing the most densely populated areas.

intertropical zone where climate is characterized by warm and wet summer conditions between October to March, and a cooler and drier winter between April to September (Bidone and Lacerda 2004). The yearly average freshwater water discharge into the Bay is 100 ± 59 m^3 s^{-1} (40 m^3 s^{-1} in winter and 190 m^3 s^{-1} in summer). This low freshwater input compared with the bay's water volume contributes to the predominance of polyhaline to euhaline waters.

The bay is one of the most polluted and eutrophic coastal systems worldwide. Approximately 7 million inhabitants discharge 25 m^3 s^{-1} of untreated domestic effluents directly into the bay (Kjerfve et al. 1997; Bidone and Lacerda 2004). Some small channels are directly connected to point source sewage discharge and contribute to the formation of permanent anoxic zones at the western margin of the Bay. Temporary hypoxic conditions also occur in the bottom waters of some internal sectors especially when water column stratification is enhanced (Paranhos et al. 1998; Ribeiro and Kjerfve 2002; Cotovicz et al. 2015). The eutrophication process started since the 1950s (Borges et al. 2009), when the human settlement increased drastically. Fluxes of phosphorous are currently 9-times higher than those estimated since the late 1800s (Borges et al. 2009), and sedimentation rates have increased up to 14-times over the last 50 yr (Godoy et al. 2012), in parallel with a 10-fold increase in the flux of organic matter to the sediments (Carreira et al. 2002). Actually, the intense eutrophication process of the bay contributes to the predominance of a strong sink of atmospheric CO_2, whereas strong CO_2 outgassing is restricted to the most polluted channel at the vicinity of the urban area (Cotovicz et al. 2015). The geomorphological configuration and physicochemical water characteristics of the bay, despite of the irregular human settlement along the watershed, only generates a moderate spatial heterogeneity of the waters properties, particularly along its main and deeper water channel.

We compartmentalized the bay into five domains (sectors 1, 2, 3, 4, and 5) as described by Cotovicz et al. (2015) for the treatment, computations and interpretation of the data (Fig. 1). Briefly, sector one (S1) corresponds to the lower portion at the mouth of the bay with a narrow and deep tidal channel, where the maximum water exchange with the coastal waters occurs. Sector two (S2), located at the western part of the bay and delimited to the north by the Governador Island, is one of the most contaminated areas of Guanabara Bay which receives sewage from Rio de Janeiro City. Sector three (S3) is a transitional area that corresponds to the deeper channel and connects the mouth of the bay (S1) with the upper more enclosed location which embeds sectors 4 and 5. Sector four (S4), located at the northeastern part of the bay, is shallow, moderately impacted and bordered by a 90 km^2 of mangrove forest. Sector five (S5) is the most confined area of the bay, located behind the Governador Island. It is shallow, presents the longest water turnover times and receives significant amounts of sewage waters. The small western channel connecting S2 and S5 was not included in this research due to its difficult access and extreme degree of contamination, but only covers less than 5% of the entire bay.

Sampling strategy

Nine sampling campaigns were conducted from April 2013 to April 2014. For each survey, discrete sampling for methane, chlorophyll *a* (Chl *a*), dissolved inorganic nutrients (nitrate, nitrite, ammonium, and phosphate) and dissolved oxygen (DO) was conducted at 16–19 stations distributed across the bay, except in December 2013, when only eight stations could be sampled in sectors 3, 4, and 5 due to logistical problems (Fig. 1). The number of stations

for each sector was chosen in accordance to the surface area (size) of each sector, their oceanographic characteristics, as well as, the degree of anthropogenic influence derived from the literature. The depths of the sampling stations ranged between 2 m and 30 m, in all averaging a depth of 5.5 m. The number of stations for each sector varied between 3 and 5. Surface water samples were collected at ~30 cm depth with a Niskin bottle model Alfakit 3L, and henceforth conditioned (i.e., fixed and/or kept on ice in the dark) for further chemical analysis in the laboratory. Vertical profiles of temperature, salinity, and DO were performed at all discrete stations with a calibrated multiparameter probe model YSI 6600 V2. The comparison between surface and bottom waters in terms of CH_4 concentrations and other parameters was only performed at some stations, during the summer period, and during conditions of maximum stratification in sectors 3, 4, and 5. The total number of concomitant surface and bottom water samples were 17, 11, and 20, in sectors 3, 4, and 5, respectively, all covering the period from Ocotber-2013 to February-2014.

Analytical procedures

Samples for dissolved methane were collected in 60 mL pre-weighted serum glass bottles, completely filled with water from a homemade sampler that limits gas exchange and prevents bubble formation (Abril et al. 2007). The bottles were sealed and preserved with saturated mercuric chloride to inhibit microbial activity. In the laboratory, a headspace was created by injecting 10 mL of N_2 into the bottles. The samples were vigorously shaken to obtain complete equilibration between air and water phases. After a period of 10–12 h, CH_4 concentrations were determined by gas chromatography (GC) with flame ionization detection (FID) (Abril et al. 2007). In situ methane concentrations were calculated using the respective volumes of water and headspace in the vial and the solubility coefficient of methane of Yamamoto et al. (1976) as a function of temperature and salinity. Reproducibility of the CH_4 analysis was generally better than 5%. Whatman GF/F filters were used for the Chl *a* analyses and the filtrate for the nutrient analyses. Dissolved inorganic nitrogen (ammonium, nitrite, and nitrate) and phosphate were quantified as in Grasshoff et al. (1999) and Chl *a* as in Strickland and Parsons (1972). All water samples were kept in the dark and on ice during transport to the respective laboratories and nutrient samples and Chl *a* filters kept at −18°C in a freezer prior to analyses. Wind velocity (U_{10}), accumulated precipitation over 7 days (the precipitation rate reaching the ground over the period of 7 d) and atmospheric temperature were recorded at the two airports of Rio de Janeiro city, Santos Dumont and Galeão, located in the outer and inner sectors of the Bay, respectively, and were kindly provided by the Brazilian Institute of Aerial Space Control (ICEA, Fig. 1).

Calculations

Diffusive fluxes of CH_4 at the air-water interface were computed with the following equation:

$$F(CH_4) = k_{g,T} \times \Delta CH_4 \quad (1)$$

with $F(CH_4)$, the diffusive flux of CH_4, $k_{g,T}$ the gas transfer velocity of a given gas (g) at a given temperature (T) and $\Delta CH_4 = (CH_{4w} - CH_{4eq})$ the CH_4 concentration gradient between the water (CH_{4w}) and the water at equilibrium with the overlying atmosphere (CH_{4eq}). The considered atmospheric partial pressure of CH_4 was 1.8 μatm, which corresponds to CH_4 concentrations (CH_{4eq}) in the range of 2.3–2.4 nmol L^{-1} due to variations in water temperature and salinity and air temperature.

The gas transfer velocity $k_{g,T}$ was computed with the following equation (Jähne et al. 1987):

$$k_{g,T} = k_{600} \times (600/Sc_{g,T})^n \quad (2)$$

where k_{600} is the gas transfer velocity normalized to a Schmidt number of 600 ($Sc = 600$, for CO_2 at 20°C), $Sc_{g,T}$ is the Schmidt number of a given gas at a given temperature (Wanninkhof 1992) and n being equal to 2/3 for wind speed < 3.7 m s^{-1} and equal to 0.5 for higher wind speed (Jähne et al. 1987; Guérin et al. 2007).

In this study, we use two empirical equations to derive the k_{600} values: the parameterization as a function of wind speed by Raymond and Cole (2001; RC01) and the parameterization as a function of wind speed, estuarine surface area and water current velocity by Abril et al. (2009; A09).

The Raymond and Cole (2001) parameterization can be calculated by the follow equation:

$$k_{600}(\text{RC01}) = 1.91\exp 0.35U_{10} \quad (3)$$

where k_{600} is the gas transfer velocity normalized to a Schmidt number of 600 expressed in cm h^{-1}, and U_{10} is the wind speed at 10 m height in m s^{-1}.

The Abril et al. (2009) parameterization can be calculated by the follow equation:

$$k_{600}(\text{A09}) = 1.80\exp -0.0165v + [1.23 + 1.00\text{LOG}(S)]U_{10} \quad (4)$$

where k_{600} is the gas transfer velocity normalized to a Schmidt number of 600 expressed in cm h^{-1}, v is the water current velocity in m s^{-1}, S is the surface area of the estuary expressed in km^2, and U_{10} is the wind speed at 10 m height in m s^{-1}. The k value of CH_4 for the in situ conditions is then calculated from Eq. 2 using the Schmidt number of a given gas at a given temperature and salinity (Wanninkhof 1992).

The RC01 and A09 parameterizations are specific for estuaries, although they have been established in macro-tidal and funnel-type estuaries, they provide, respectively, k_{600} values 12% and 70% higher than those predicted by the oceanic parameterization (Wanninkhof 1992) for a wind speed of

Table 1. Mean, standard deviation, minimum, and maximum values of the main physico-chemical water properties of Guanabara Bay, for each sector and season.

	Winter					Summer				
	Sector 1	**Sector 2**	**Sector 3**	**Sector 4**	**Sector 5**	**Sector 1**	**Sector 2**	**Sector 3**	**Sector 4**	**Sector 5**
Temp. (°C)	23.0 ± 0.9	24.7 ± 0.9	23.9 ± 1.1	25.4 ± 2.6	25.2 ± 1.6	24.4 ± 2.3	27.3 ± 2.7	27.1 ± 1.9	28.9 ± 1.2	28.3 ± 2.3
	24.4–22.0	23.1–26.5	22.6–26.8	22.5–31.3	23.2–28.8	21.6–28.9	23.3–32.2	24.3–30.9	26.5–31.0	24.3–33.6
Sal.	32.2 ± 2.2	30.7 ± 1.7	29.9 ±3.2	26.9 ± 5.3	27.3 ± 4.7	32.5 ± 1.7	28.3 ± 3.6	29.4 ± 3.0	26.2 ± 3.1	27.2 ± 3.2
	26.3–34.0	26.8–33.0	21.5–32.8	15.6–31.7	18.1–32.7	28.8–34.6	20.0–33.5	22.3–33.5	19.9–30.8	19.6–32.1
DO (%)	87 ± 9	72 ± 35	112 ± 25	153 ± 71	157 ± 69	115 ± 30	141 ± 90	158 ± 48	155 ± 48	166 ± 71
	69–105	10–148	74–164	57–336	54–278	68–221	4–263	61 – 357	83–361	66 – 370
Chl *a* (μg L^{-1})	11 ± 7	25 ± 43	27 ± 19	52 ± 44	78 ± 73	24 ± 31.61	122 ± 93	85 ± 69.41	76 ± 60	86 ± 61
	2–37	3–200	74–164	4–162	6–324	2–126	4–279	1–537	17–288	8–822
NO_3^--N (μmol L^{-1})	4.85 ± 3.58	5.85 ± 5.58	6.60 ± 6.12	3.12 ± 3.75	2.67 ± 2.32	1.31 ± 1.11	0.84 ± 0.75	1.32 ± 1.36	0.26 ± 0.19	0.89± 0.88
	0.34–12.54	<DL - 18.69	0.16–19.13	<DL - 14.74	0.04–9.20	0.13–3.66	0.02–2.56	0.18–5.31	0.07–0.78	0.04–3.66
NO_2^--N (μmol L^{-1})	2.10 ± 2.22	3.52 ±3.44	2.80± 3.24	2.26 ± 3.19	2.09 ± 2.25	0.73 ± 0.70	1.33 ± 1.10	0.77± 0.86	0.07 ±0.04	1.11 ± 1.29
	0.12–7.30	0.10–10.67	0.12–10.79	0.03–9.37	0.03–7.08	0.06–2.28	0.13–4.36	0.00–2.53	0.03–0.13	0.05–3.82
NH_4^+-N (μmol L^{-1})	10.20 ± 5.94	45.53 ± 22.68	14.32 ± 9.87	6.78 ± 3.28	35.58 ± 30.34	4.78 ± 5.40	34.84 ± 27.93	3.56 ± 4.95	1.76 ± 3.28	12.70 ± 14.60
	1.40–22.50	11.51–94.73	0.26–37.96	0.04–29.29	0.36–130.12	0.60–18.27	0.15–70.30	0.04–15.17	0.11–11.72	0.13–53.75
PO43$^-$-P (μmol L^{-1})	1.33 ± 0.53	5.51± 2.43	1.31 ± 0.84	0.98 ± 0.66	2.67 ± 2.55	0.76 ± 0.57	4.97 ± 5.36	1.73 ± 1.28	1.32 ± 0.98	1.52 ± 1.10
	0.56–2.45	2.62–10.22	0.19–2.76	0.03–2.38	0.04–8.72	0.11–2.12	0.17–20.79	0.17–4.10	0.2–2.96	0.02–3.90
pCO_2* (μatm)	542 ± 81	999 ± 578	404 ± 103	296 ± 252	352 ± 339	329 ± 115	564 ± 840	124 ± 77	160 ± 107	149 ± 93
	400–662	417–2500	184–559	53–1140	80–1390	130–507	67–3000	47–364	53–437	24–411
CH_4 (nmol L^{-1})	147 ± 116	1634 ± 2844	155 ± 86	182 ± 201	292 ± 223	193 ± 146	2185 ± 3717	177 ± 130	100 ± 39	307 ± 261
	19–568	73–10,350	59–358	57–963	67–725	62–559	110–11,803	40–456	45–180	42–882

temp., temperature; sal., salinity; DO, dissolved oxygen; Chl *a*, chlorophyll *a*; NO_3^--N, nitrate; NO_2^--N, nitrite; NH_4^+-N, ammonium; PO_4^{3-}-P, phosphate; pCO_2, pressure partial of CO_2; CH_4, methane; DL, detection limit.
*Data from Cotovicz et al. (2015).

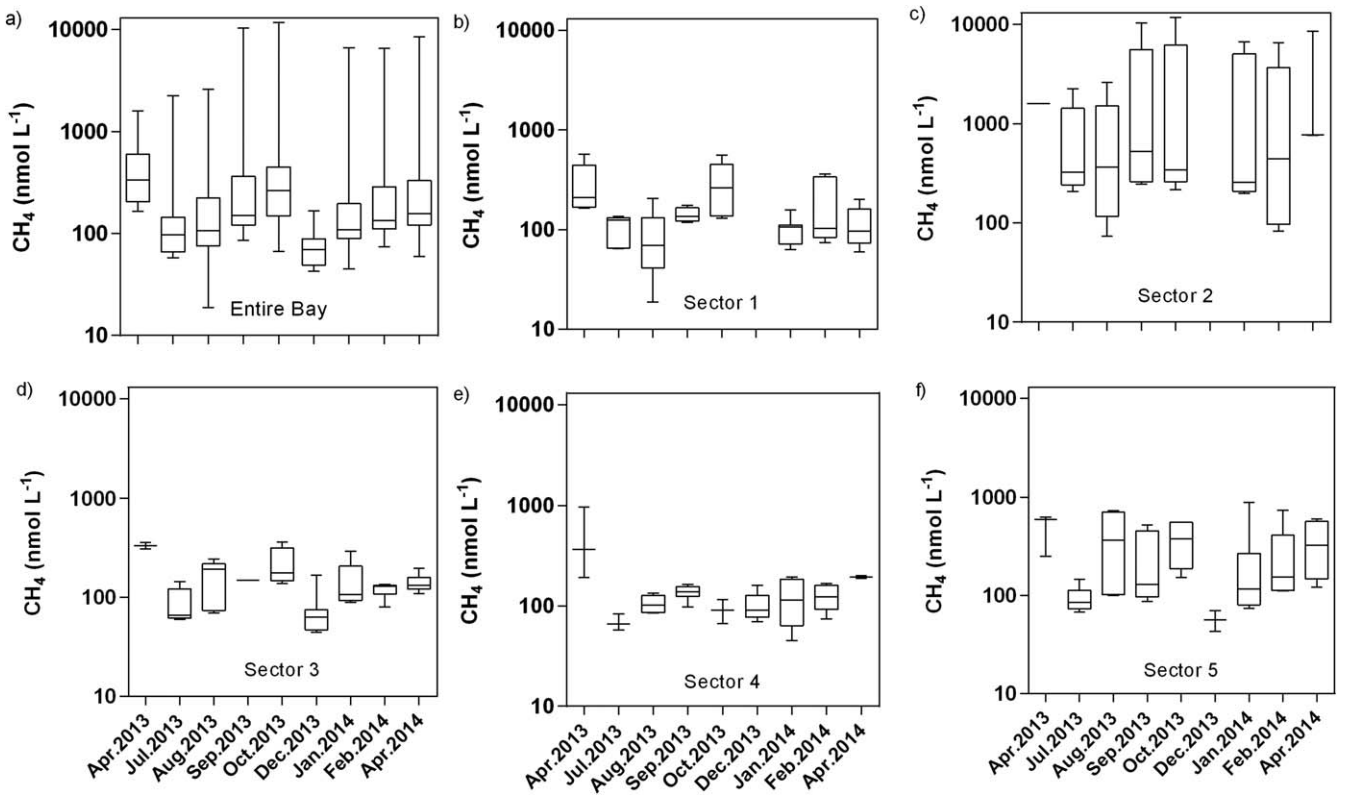

Fig. 2. Box plots (maximum, percentile 75%, median, percentile 25% and minimum) of CH_4 concentrations for all sampling campaigns (**a**) and for each individual sector 1–5 (**b**, **c**, **d**, **e** and **f**). Note that graphs are in logarithm scales.

5 m s^{-1}. The coefficient of Raymond and Cole (2001) is based on tracer injections applied in nine rivers and estuaries and can be considered the more conservative estimative, whereas the coefficient of Abril et al. (2009) is based on chamber measurements in seven estuaries, and accounts for the current velocity effect in addition to wind and gives higher *k* values. Wind speed data was logged every hour and averaged at 12 h intervals throughout the sampling days. The 12 h averages were henceforth integrated over the entire sampling season. According to Cotovicz et al. (2015), average k_{600} values based on 15 min wind speed were not significantly different from k_{600} based on 12 h average wind speed, suggesting that short storms had a negligible impact on daily integrated gas transfer velocities. We used values of tidal-average current velocity per sector as described in Kjerfve et al. (1997). In Guanabara Bay, the impact of current velocity on the k_{600} calculated with the A09 equation was only about 2% at maximum current velocity close to the bay outlet, were current velocities were 0.6–0.8 m s^{-1} on average (Kjerfve et al. 1997). The fluxes were calculated for each sector and for each sampling campaign, separating nighttime (campaigns conducted before 09:30 a.m.) and daytime (campaigns conducted after 09:30 a.m.) periods to account for the diel wind patterns as described in Cotovicz et al. (2015), and then integrated over the entire sampled period. The CH_4 fluxes calculated with each equation were expressed in μmol m^{-2} d^{-1} in each sector. To compare the air-water fluxes of CH_4 with those of CO_2 (Cotovicz et al. 2015) and N_2O (Guimarães and de Mello 2008) we used the concepts of global warning potential (GWP), by considering that 1 g of CH_4 and N_2O have a GWP equivalent of 28 g and 268 g of CO_2, respectively, on a 100 yr basis (IPCC 2013).

Statistical analysis

Tests for the normal distribution of the data were carried out with the Shapiro–Wilk test. As the tests not presented normal distributions for the data set, we used the non-parametric Wilcoxon test to compare the average values between deep and surface waters composition, as well as for seasonal differences. The calculations of correlations between accumulated precipitation of 7 d (mm), wind velocity (cm s^{-1}), dissolved oxygen (DO; %), Chl *a* (μg L^{-1}), aquatic partial pressure of CO_2 (pCO_2; μatm), salinity, temperature (°C), and CH_4 (nmol L^{-1}) were performed with the Spearman rank coefficient analysis. For the Principal Component Analysis (PCA) calculation, we started with a correlation matrix presenting the dispersion of the original variables (data were normalized by *z*-scores with average data for each sampling campaign), that was utilized to extracting the eigenvalues and eigenvectors. Thereafter, the principal components were obtained by multiplying an eigenvector, by the original

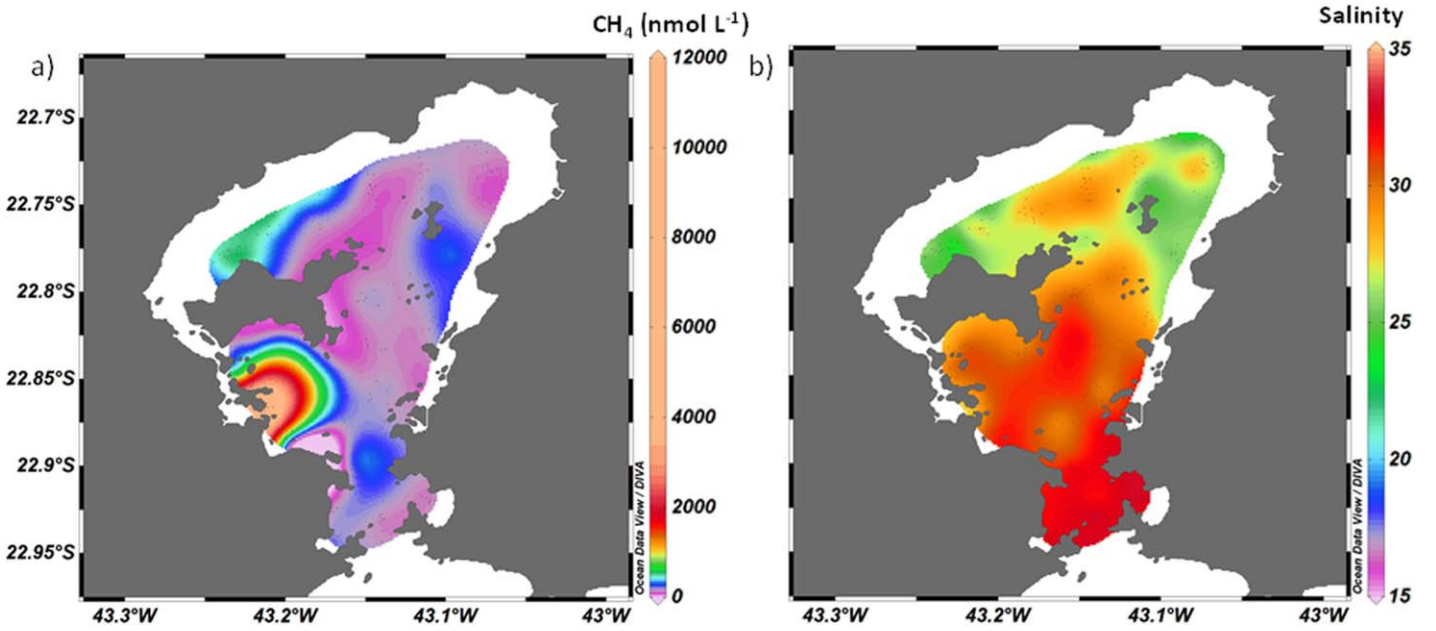

Fig. 3. Composite maps showing the spatial distributions of the CH_4 concentrations (**a**) and salinity (**b**) in surface waters of the Guanabara Bay for all sampling periods.

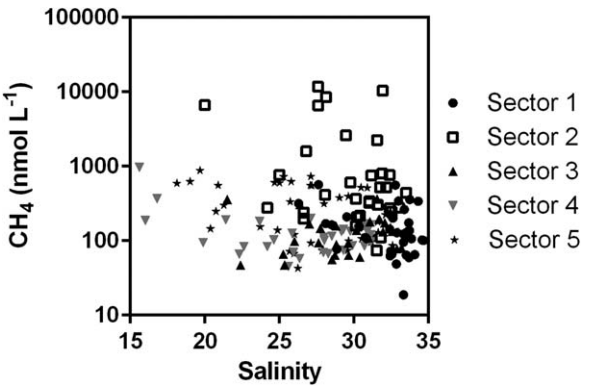

Fig. 4. Relationship between CH_4 concentrations and salinity for each sector of Guanabara Bay.

correlated variables. The pCO_2 and photosynthetically active radiation (PAR) values in the PCA were obtained from the published paper of Cotovicz et al. (2015). All statistical analysis were based on $\alpha = 0.05$. We used the STATISTICA 7.0 program (STATISTICA software, StatSoft, Inc., Tulsa, Oklahoma) to perform all PCA steps and the GraphPad Prism 6 program (GraphPad Software, Inc., La Jolla, California) to perform the other statistical tests.

Results

The air temperature showed a seasonal trend and the precipitation regime abided to a unimodal seasonal pattern similar to the longer term historical record (with exceptions of December-2013 and January-2014 that were exceptionally warmer and drier). The average air temperature in summer was 26.3°C (October-2013 to March-2014) and in winter was 22.3°C (April-2013 to September-2013). More details about the climatological conditions for the sampled period are available in Cotovicz et al. (2015). Table 1 shows the results of the principal physico-chemical properties of the waters in Guanabara Bay, separated for the five sectors and for the winter and summer seasons. The variations of salinity and water temperature averaged by sectors varied along the bay between 27.0–32.2, and 23.8–26.8°C, respectively. In general, in the upper sectors of the bay (S4 and S5), the salinities were lower and temperatures were higher. The sector closest to the entrance of the bay (S1), showed the lowest temperatures and highest salinities, with small seasonal variations.

All sampling points of Guanabara Bay showed water methane concentrations higher than the atmospheric concentrations. The supersaturated conditions indicated that Guanabara Bay is a permanent source of CH_4. The sector-averaged methane concentrations exhibited marked spatial heterogeneity between the sectors (Table 1; Fig. 2). Figure 3 shows a map with the spatial distribution of methane and salinity for the entire data set. Highest CH_4 concentrations occurred in S2 in the western part of the bay and were not associated with lower salinities. Some high CH_4 concentrations (although lower than in S2) also occurred in the S4 and S5, being consistent with lower salinities. Figure 4 shows the relationship between CH_4 concentrations and salinity. Only S5 showed a significant and inverse correlation of CH_4 and salinity ($r = -0.40$; $p < 0.01$; Spearman correlation). For

Table 2. Comparison between surface and bottom waters for temperature, salinity, DO, NH_4^+-N, and CH_4 (average concentrations ± standard deviation; $n = 43$).

	Temperature*** (°C)	Salinity***	DO*** (%)	Chl *a*** (μg L^{-1})	NH_4^+-N* (μmol L^{-1})	CH_4 (nmol L^{-1})
Surface water	26.0 ± 2.8	29.3 ± 3.8	128 ± 58	62 ± 68	7.6 ± 12.3	150 ± 132
Bottom water	22.1 ± 2.7	33.0 ± 2.4	53 ± 23	10 ± 12	12.8 ± 11.5	134 ± 58

*Significant difference between surface and bottom waters (Wilcoxon test; $p < 0.05$).
**Significant difference between surface and bottom waters (Wilcoxon test; $p < 0.001$).
***Significant difference between surface and bottom waters (Wilcoxon test; $p < 0.0001$).

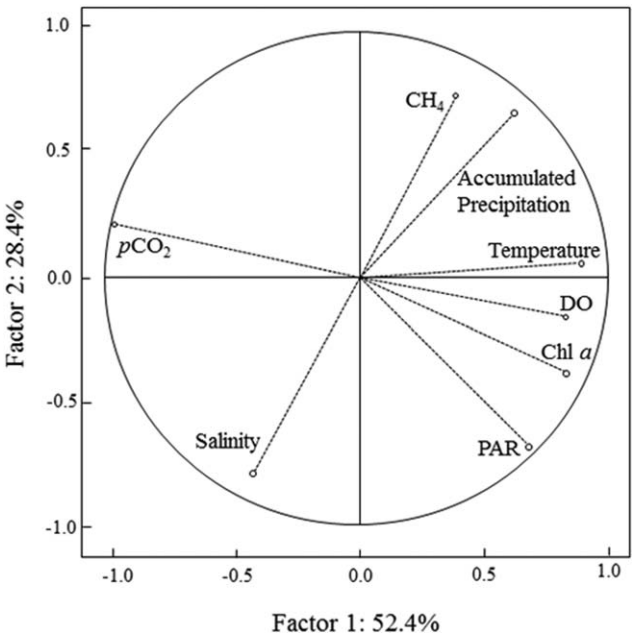

Fig. 5. Bi-dimensional plot of factor 1 and factor 2 obtained by Principal Component Analysis (PCA) using averaged data for each sampling campaing for CH_4, pCO_2, DO, Chl *a*, temperature, salinity, PAR, wind velocity and accumulated precipitation of 7 d. pCO_2 and PAR data are from Cotovicz et al. (2015).

the whole bay, the averaged concentration of CH_4 was 430 ± 1355 nmol L^{-1}, and saturation levels were 25,929% ± 77,032% (note the strong standard deviation due to both temporal and spatial variation inside the sector). The minimum and maximum concentrations of CH_4 were 18.8 nmol L^{-1} and 11,803 nmol L^{-1}, and saturation states were 948% and 606,884%, respectively. The CH_4 concentrations were not prone to significant seasonal differences ($p > 0.05$, Wilcoxon Test), with average bay concentrations of 437 ± 1278 and 426 ± 1448 nmol L^{-1} in winter and summer, respectively. Sector 2, that is under a large and direct influence of sewage discharge, showed highest CH_4 values with an annual average of 1858 ± 3181 nmol L^{-1}. S5, which is under influence of discharge of small and polluted rivers, attained an annual average of 298 ± 236 nmol L^{-1} and a maximum concentration of 882 nmol L^{-1}. The other three sectors presented similar methane concentrations, with annual average values of 169 ± 129, 140 ± 82, and 149 ± 160 nmol L^{-1} for, S1, S3, and S4, respectively.

We tested the influence of accumulated precipitation on CH_4 concentration distributions. The distinction between the dry and wet conditions was made using the accumulated precipitation during 7 d before each sampling campaign. If the accumulated precipitation of 7 d was < 15 mm the sampling campaigns conditions were considered dry (July-2013, August-2013, September-2013, and December-2013) and if the accumulated precipitation of 7 d was > 15 mm the sampling campaigns were considered to be representative of wet conditions (April-2013, October-2013, January-2014, February-2014, and April-2014). Considering the overall data set, the CH_4 concentrations showed high significant differences between dry and wet conditions ($p < 0.001$, Wilcoxon Test), with average concentrations of 324 ± 1125 and 513 ± 1513 nmol L^{-1}, respectively.

Table 2 presents the comparison between surface and bottom waters for CH_4, ammonium (NH_4^+-N), temperature, salinity, and DO concentrations, in S3, S4, and S5 during the summertime period. The differences between surface and bottom waters for CH_4 values were not significant ($p > 0.05$, Wilcoxon Test), with mean concentrations of 150 ± 132 and 134 ± 58 nmol L^{-1}, respectively. However, the temperature, salinity, DO, and NH_4^+-N concentrations showed highly significant differences between surface and bottom waters ($p < 0.001$; Wilcoxon Test; Table 2). No vertical variation occurred in CH_4 concentrations, although water column stratification occurred particularly in these sectors of the bay during summer. It must be kept in mind that bottom water samples were not collected at all stations and campaigns, which explains why these average values for the period are different from those of the entire data set.

Results of the principal component analysis (PCA) are shown in Fig. 5 and included the parameters of temperature, salinity, DO, Chl *a*, PAR, wind velocity, accumulated precipitation of 7 d, pCO_2 and CH_4. The factors 1 and 2 together explain for about 80% of the data variance. Factor 1, that explains 52.4% of the data variance, is dominated by CO_2 in one hand and by DO, Chl *a* and temperature on the other hand. Factor 2, that explains about 28.4% of the data variance, shows the influence of CH_4 and salinity, and also the accumulated precipitation of 7 d. The PCA and correlations

Table 3. Spearman correlation matrix for accumulated precipitation of 7 d (Accum Prec 7; mm), wind velocity (Wind; cm s^{-1}), dissolved oxygen (DO; %sat), chlorophyll *a* (Chl *a*; μg L^{-1}), pCO_2 (μatm), salinity, temperature (Temp; °C) and CH_4 (nmol L^{-1}) in the Guanabara Bay. The values were established with averages for each sampling campaign. The values of pCO_2 were included from the data published by Cotovicz et al. (2015).

	Accum Prec 7	Wind	DO	Chl *a*	pCO_2	Salinity	Temp	CH_4
Accum Prec 7		0.29	0.47	0.43	−0.46	−0.55	0.27	0.81*
Wind	0.29		0.88**	0.83**	−0.91**	−0.08	0.66	−0.13
DO	0.47	0.88**		0.76*	−0.93**	−0.36	0.76	−0.10
Chl *a*	0.43	0.83**	0.76*		−0.85**	−0.06	0.60	−0.01
pCO_2	−0.46	−0.91**	−0.93**	−0.85**		0.38	−0.86**	0.05
Salinity	−0.55	−0.08	−0.36	−0.06	0.38		−0.43	−0.08
Temp	0.27	0.66	0.76*	0.60	−0.86**	−0.43		0.01
CH_4	0.82*	−0.13	−0.10	−0.01	0.05	−0.08	0.01	

*Correlations significant at $p < 0.05$.
**Correlations significant at $p < 0.01$.

Table 4. Annual average concentrations of CH_4, current velocity, wind velocity (U_{10}), gas exchange velocity (k_{600}) and CH_4 fluxes calculated according to Raymond and Cole (2001) (RC01) and Abril et al. (2009) (A09) for each sector (1–5) and integrated for entire superficial area. Note that for CH_4 concentrations we presented the average, standard deviation, minimum and maximum values.

	CH_4 (nmol L^{-1})	Current velocity (m s^{-1})*	U_{10} (m s^{-1})	k_{600} (cm h^{-1})		CH_4 flux (μmol m^{-2} d^{-1})		CH_4 flux (t C CH_4 d^{-1})	
				RC01	A09	RC01	A09	RC01	A09
Sector 1 (47 km^2)	169 ± 129 (18–568)	0.6	3.1	6.6	10.6	291	454	0.16	0.26
Sector 2 (32 km^2)	1858 ± 3181 (73–11,803)	0.6	2.8	5.3	9.8	2583	4798	0.99	1.89
Sector 3 (96 km^2)	140 ± 82 (40–364)	0.6	3.2	6.6	10.7	296	444	0.34	0.51
Sector 4 (55 km^2)	149 ± 160 (45–963)	0.3	2.7	5.4	8.8	242	394	0.16	0.26
Sector 5 (80 km^2)	298 ± 236 (42–882)	0.3	2.7	5.2	8.8	463	807	0.44	0.77
Entire Bay (310 km^2)	430 ± 1353 (18–11,803)					565	980	2.10	3.65

*According to Kjerfve et al. (1997).

matrix consistently reveal that the controlling processes over CH_4 and CO_2 are different and not linked. Table 3 summarizes the results of the Spearman correlations performed with the average concentrations, per campaign, with the same variables utilized for the PCA analysis. The results of the PCA and the Spearman correlation analysis were very consistent. Methane concentrations were shown to be positively correlated with the accumulated precipitation of 7 d, whereas the CO_2 concentrations were strongly and inversely correlated with DO, Chl *a*, PAR and wind velocity (Cotovicz et al. 2015).

Table 4 shows the annual calculated fluxes of CH_4 at the air-water interface for Guanabara Bay. Note that the fluxes were computed taking into account two different estuarine-specific gas exchange coefficients as described in the methodology section (Raymond and Cole 2001; Abril et al. 2009). Sector 2 exhibited the highest CH_4 fluxes (2583–4798 μmol m^{-2} d^{-1}) responding approximately to half of the total bay emissions, despite of its smallest surface area as compared with the other sectors. Second highest CH_4 fluxes were observed in S5 (463–807 μmol m^{-2} d^{-1}). Sector 3 showed higher fluxes than sectors S1 and S4, despite of the little differences between the calculated emissions of these sectors. For the entire bay, the calculated fluxes were 565 μmol m^{-2} d^{-1} and 980 μmol m^{-2} d^{-1} for the gas transfer velocities of RC01 and A09, respectively. The total CH_4 emissions of Guanabara Bay were between 2.10 and 3.65 t C-CH_4 d^{-1}.

Discussion

Origin of dissolved CH_4 in Guanabara Bay

Methane concentrations in estuarine waters results from the balance between dissolved CH_4 advection with water masses (input and output) and CH_4 production, oxidation, and degassing (Borges and Abril 2011). With respect to production, the bacterial mineralization of sedimentary organic matter occurs following a sequence of reactions, which starts with aerobic decomposition and ends with methanogenesis,

the latter taking place when all electron acceptors are depleted (Martens and Berner 1974). CH_4 production is estuarine waters greatly depends on salinity and organic matter sedimentation rate (Borges and Abril 2011). Gas bubble formation in the sediment is favoured by high sedimentation rates and low salinity and sulphate availability. In estuaries, the transport of these bubbles through the water column is controlled by variations in hydrostatic pressure with the tide (methane transported in gas bubbles generally escapes oxidation) (Martens and Klump 1980; Middleburg et al. 1996; Borges and Abril 2011). Generally the fraction of these CH_4 bubbles that dissolves in the water column is minor and the presence of gas bubbles in the sediment is not necessarily related to high dissolved CH_4 concentrations in surface waters. Microbial losses of CH_4 in estuaries include anaerobic and aerobic microbial oxidation processes, whose intensity depend on the concentration of available CH_4 and potential oxidants and their transport in waters and sediments, as well as environmental factors that directly affect microbial activity such as temperature, salinity, and turbidity (Borges and Abril 2011).

Despite the fact that CH_4 production has been reported in gassy coastal sediments found in shallow and productive environments where methane production might occur near the sediment-water interface (Martens et al. 1998), most studies converge to the conclusion that high-CH_4 waters are restricted to the low salinity estuarine zones (Upstill-Goddard et al. 2000; Middelburg et al. 2002; Biswas et al. 2007; Chen et al. 2008; Zhang et al. 2008; Zhou et al. 2009; Dutta et al. 2015). Indeed, a general seaward decrease has been observed for dissolved CH_4 concentrations and air-water diffusive fluxes (Upstill-Goddard et al. 2000; Middelburg et al. 2002) and sediment-water CH_4 fluxes (Kelley et al 1990), as well as sediment-air fluxes at low tide in intertidal areas (Bartlett et al. 1987; Borges and Abril 2011). The simple model of Martens et al. (1998) quantitatively describes how total organic carbon remineralization rates can be divided between sulphate reduction and methane production as a function of both organic carbon sedimentation and degradation rates. According to this model developed for coastal and marine sediments, in saline environments where sulphate is available, methanogenesis starts to be significant only when the organic carbon sedimentation rate exceeds about 35 mol C m^{-2} yr^{-1} (Martens et al. 1998).

Beside the eutrophic status of Guanabara Bay and the fact that it behaves as a CO_2 sink (Cotovicz et al. 2015), the average flux of total organic carbon to the sediments was much lower than this value (about 25 mol C m^{-2} yr^{-1}; Carreira et al. 2002) and thus not sufficient to sustain marked CH_4 production in the sediments. In addition, the sedimentation rates of Guanabara Bay (mean of 1–2 cm yr^{-1}, Godoy et al. 2012) are considerably lower than those reported in gassy organic-rich coastal sediments (i.e., >10 cm yr^{-1}; Martens and Klump 1980). Because of the overall high salinity, the production of methane in Guanabara Bay probably occurs much deeper in the sediment, and this CH_4 can be subject to an almost complete anaerobic CH_4 oxidation at the sulphate–CH_4 transition, which prevents CH_4 from diffusing upward (Martens and Berner 1977; Blair and Aller 1995). This is probably why we found no significant differences in CH_4 concentrations between bottom and surface waters, even in the most confined S4 and S5 and during maximal stratification of the water column at daytime in summer. In these conditions, other parameters such as oxygen, Chl *a*, DO, and NH_4^+-N did show marked vertical gradients (Table 2) induced by photosynthesis, respiration and sediment-water fluxes (Cotovicz et al. 2015). The significantly higher NH_4^+-N concentrations in bottom waters compared with surface waters ($p < 0.01$, Wilcoxon Test), indicates significant diffusion from anoxic sediments and the occurrence of anaerobic processes other than methanogenesis, such as sulphate reduction.

In Guanabara Bay, the spatial distribution of CH_4 clearly indicates a major source due to sewage discharge near the harbour of Rio de Janeiro (Fig. 3), which generates the highest CH_4 concentrations in S2 all year long (Fig. 2). This area of high CH_4 concentrations in polyhaline waters also showed high CO_2 and NH_4^+-N, and low pH and DO concentrations (Cotovicz et al. 2015). Other CH_4 maxima occurred in S4 and S5, close to the mouths of small rivers, being concomitant with lower salinities (Fig. 3). This spatial distribution suggests that the dissolved CH_4 in Guanabara Bay largely originates from the sewage network (in S2) and from polluted rivers (in S4 and S5), and much less from the internal benthic carbon recycling of phytoplankton and/or sewage derived material. Because of this major source of CH_4 from sector 2, Guanabara Bay does not follow the general pattern of seaward decrease of dissolved CH4 concentrations observed in others estuaries worldwide. The weak relationship between salinity and CH_4 (Fig. 4) indicates that CH_4 is readily dispersed in the estuarine system at relatively high salinities, as the distance of the fresh water source and estuarine mixing zone is very short. This is confirmed by the spatial distributions of CH_4 and salinity for the whole sampling period (Figs. 3, 4). These CH_4 distributions also suggest that maybe a fraction of the labile domestic organic matter does not disperse over the entire bay, but deposits rather rapidly in the most polluted confined anoxic areas of the bay, where it is degraded anaerobically to CH_4.

It is probable that methane production can occur near the highly polluted and very shallow saline waters (< 1 m) and/or intertidal zones close to the urban areas (i.e., western area of the bay, see Fig. 1) which could not be sampled for logistic reasons, but that potentially receive high organic carbon inputs. This sector of the bay is close to the urban area where sewage outlet has been described as hypoxic to anoxic, heavily polluted with organic matter and dissolved inorganic nutrients (Paranhos et al. 1998; Ribeiro and Kjerfve

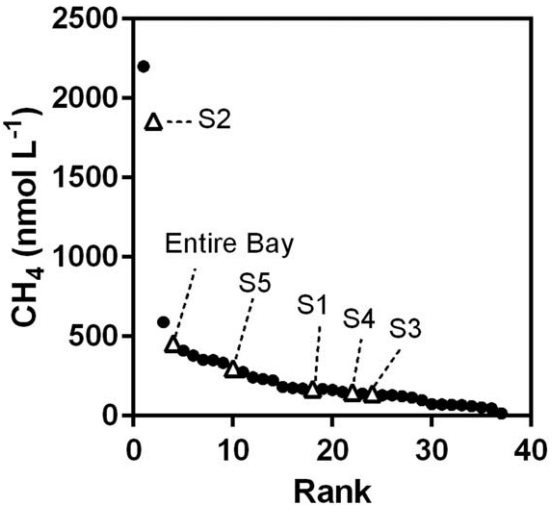

Fig. 6. Rank of averaged dissolved CH_4 concentrations (nmol L^{-1}) in estuarine environments (black dots), including the results for the entire Guanabara Bay and it's sectors (triangles). Data compiled from the literature as reported in Supporting Information 1.

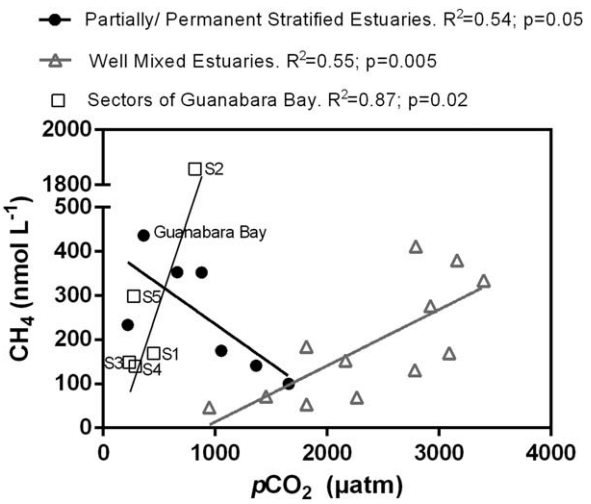

Fig. 7. Average CH_4 dissolved concentrations (nmol L^{-1}) vs. average partial pressure of CO_2 (pCO_2 in μatm) in 19 estuarine systems. This figure was adapted from Borges and Abril (2011). The Supporting Information 2 presents the included systems and references.

2002) and is subject to the highest values of bacteria and virus abundances (Fistarol et al. 2015). Previous studies reported that this inner portion of the bay presented bacterioplankton taxonomic sequences closely related to methanogenic archaea (Vieira et al. 2007; Turque et al. 2010). Ebullition in these very polluted shallow areas might also be significant (Nirmal Rajkumar et al. 2008), particularly at low tide, but could not be quantified in this study. It is thus assumed that the CH_4 is transported in dissolved form from these polluted channels to the centre of the bay where it progressively degasses to the atmosphere. Such transport mechanisms explains the correlation between CH_4 concentration and 7-d accumulated precipitation (Table 3; Fig. 5) that favours methane inputs from lateral advection. Further, these mechanisms could explain the weak correlation between CH_4 and salinity as a large fraction of the methane production can occur in highly polluted saline waters.

In an Indian estuary, Nirmal Rajkumar et al. (2008) also reported a similar spatial variability independent of salinity due to strong environmental pollution. In a polluted estuary in Spain, Burgos et al. (2015) also found a positive relationship between precipitation and CH_4 concentrations due to wastewater discharge. In Guanabara Bay, a saline and moderately stratified system, the in situ production of CH_4 in the bay itself appears minor, in spite of the high levels of eutrophication. It should also be noted, that contrary to other sites elsewhere (Barnes et al. 2006; Biswas et al. 2007; Ramesh et al. 2007; Dutta et al. 2015), we found no clear enrichment of CH_4 in the water of the sector close to a mangrove forest located in the northeastern part of Guanabara Bay (Figs. 2, 3). As also observed for CO_2 (Cotovicz et al. 2015), export of CH_4 from the mangroves does not seem to be important in Guanabara Bay. Although we could not sample the shallowest waters at the vicinity of the flooded forest, the transport by tidal pumping from the upper mangrove forest itself appears to be governed by slow advective processes, due to the microtidal character of the Bay (average tidal amplitude 0.7 m).

Comparison of CH_4 concentrations and emissions patterns from other estuaries

Comparative studies conducted between pristine and impacted sites reveal higher methane concentrations at human-impacted estuaries (Kristensen et al. 2008; Allen et al. 2010). The averaged and some extreme methane concentrations in Guanabara Bay are well above those reported in most estuaries worldwide (Supporting Information 1, 2 and 3). Figure 6 shows an estuarine ranking of CH_4 concentrations compiled from published data. Guanabara Bay presented the third highest CH_4 estuarine water concentrations worldwide. If we consider the most polluted sector of Guanabara Bay (S2), only two estuaries showed average concentrations close to ours (Adyar river estuary, Nirmal Rajkumar et al. 2008 and Guadalete river estuary, Burgos et al. 2005). These two estuaries are drowned river valley, funnel-type estuaries, with a spatially well-defined salinity gradient and receive sewage waters in their low salinity areas, which potentially favour in situ methane production. If we consider marine-dominated estuaries with high salinity waters, such as Guanabara Bay, the CH_4 concentrations in Guanabara Bay are higher than those reported in the literature so far.

Analysing the types of estuarine systems (Supporting Information 3), we did not find clear higher emissions of CH_4 in the tropics. The scarce number of studies conducted in tropical estuaries (less than 20% of the references cited in

the Supporting Information 3) unable us to cover this knowledge-gap with high degree of confidence. In the tropical studies, we can observe high (Nirmal Rajkumar et al. 2008; Koné et al. 2010) and low (Zhou et al. 2009) CH_4 concentrations, depending mainly on the hydro-geomorphological conditions of the study sites, as well as the degree of human influence. In Guanabara Bay, for example, the higher emissions of CH_4 seems to be more related to the strong anthropogenic influence than the tropical climatic condition. Indeed, tropical regions present the major part of the developing countries, which are prone to high population growth rates and low sewage treatment facilities. Both of these conditions are likely to contribute to higher CH_4 emissions as also shown for Guanabara Bay.

The cross-system comparison of pCO_2 and CH_4 in estuaries also provides information regarding the role of physical and biogeochemical settings in the control of organic carbon cycling and production of CO_2 and CH_4 (Fig. 7 and Supporting Information 2). According to the analysis of Borges and Abril (2011), there is a positive relationship between CH_4 and pCO_2 in well-mixed estuarine systems, and a marked negative relationship in stratified estuarine systems. In well-mixed systems, CH_4 and CO_2 are largely derived from the degradation of allochtonous organic matter in soils and salt-marsh sediments and are then transported to the estuary. In stratified systems, autochtonous organic matter is produced by phytoplankton, consuming CO_2 in surface waters, and transferring organic matter across the pycnocline and promoting anoxic conditions in bottom layers favourable for methanogenesis in the sediments (Fenchel et al. 1995; Koné et al. 2010). Methane can then diffuse to surface waters and lead to high CH_4 concentrations. Figure 7 illustrates that Guanabara Bay occupies an extreme position with low pCO_2 (Cotovicz et al. 2015) and high CH_4 concentrations (360 μatm and 436 nmol L^{-1}, respectively). Despite the fact that Guanabara Bay is a large partially stratified system, stratification is not strong enough to maintain a permanent anoxic bottom layer such as observed for the Aby and Tendo lagoons (Ivory Coast; Koné et al. 2010) or the Mariager Fjord (Denmark; Fenchel et al. 1995). As such we believe that in situ methanogenesis sustained by phytoplankton production is not important in our sampled area and CH_4 mainly originated from lateral inputs. This statement is based on three observations that indirectly support such hypothesis. It is not based on direct measurements of methane production (or methane concentrations) in the sediment, which remains to be investigated. However, it is based on: (1) the model by Martens et al. (1998) that predicts less than 10% of methanogenesis at the average organic carbon burial rates observed in Guanabara Bay (about 25 mol C m^{-2} yr^{-1}; Carreira et al. 2002); (2) the model of Martens et al. (1998) also predicts important methanogenesis at sedimentation rates very higher than that reported in Guanabara Bay; (3) the correlation of CH_4 with accumulated precipitation, rather than with photosynthetically active radiation (PAR) and temperature, factors that enhance phytoplanktonic production. Indeed, when analysing the different sectors of Guanabara Bay separately, we observe a positive relationship between pCO_2 and CH_4 indicating a common source, i.e., sewage derived organic carbon degradation.

Calculated methane fluxes and impact on the greenhouse gas budget

The highest CH_4 degassing occurred in S2. Despite the fact that this sector occupies only approximately 10% of the sampled area, it accounts for about 50% of the total emissions showing the sewage discharge as one hotspot in the CH_4 degassing. This highlights the irregular and heterogeneous emissions of methane in Guanabara Bay, as also reported in other estuaries (Call et al. 2015; Maher et al. 2015). Comparing emissions of this sector with the reported fluxes in the literature shows that Guanabara Bay exhibits one of the highest estuarine emissions worldwide (Supporting Information 3). Barnes et al. (2006) speculated that mangrove-dominated systems could dominate coastal CH_4 emissions along the world coastal zone. However, as we see for Guanabara Bay and other estuaries, the principal source of CH_4 for coastal areas can be the polluted waters. Guanabara Bay showed emissions higher than those reported for mangrove waters (Supporting Information 3). The polluted waters of Guanabara Bay also presented some CH_4 concentrations (11,803 nmol L^{-1}) that can be even higher than the mangrove pore water CH_4 concentrations encountered in Sundarbans estuary (Biswas et al. 2007; Dutta et al. 2015).

The drivers and controls of two of the most important greenhouse gases (CO_2 and CH_4) are very different for Guanabara Bay (Table 3; Fig. 5). On the one hand, CO_2 is governed by the hydrology (temporal stratification), high availability of nutrients and photosynthetically active radiation (Cotovicz et al. 2015). These conditions promote the development of dense phytoplankton blooms and a strong annual CO_2 sink (Cotovicz et al. 2015). Conversely, the CH_4 dynamics are controlled mainly by the precipitation regime and the pollution in the watershed. When the precipitation is high, the runoff of dissolved CH_4 is enhanced and the methane concentration in the waters of the bay increases. The eutrophication process in Guanabara Bay tends to promote net CO_2 uptake (Cotovicz et al. 2015), whereas for CH_4 the strong pollution in S2 seems to reinforce the emission. Guanabara Bay is also a source of atmospheric N_2O, another important greenhouse gas, which showed highest concentrations in the polluted sectors of the bay (S2 and S5), and an average flux between 0.5 μmol m^{-2} d^{-1} and 5.1 μmol m^{-2} d^{-1} (Guimarães and de Mello 2008).

We used the concepts of global warming potential (GWP) and CO_2-equivalent emissions (CO_2-eq) (IPCC 2013) to compare the fluxes of CH_4 with those of CO_2 (Cotovicz et al. 2015) and also those of N_2O published by Guimarães and de Mello (2008) at air-water interface in Guanabara Bay. These

concepts allow us to account for the fluxes of different greenhouse gases on a common scale. We considered the last IPCC report (IPCC 2013), which provides the GWP for CH_4 and N_2O of 28 and 268, respectively (1 g of CH_4 = 28 g of CO_2; 1 g of N_2O = 268 g of CO_2; assuming a time horizon of 100 yr). After converting to CO_2-equivalent emissions our diffusive CH_4 fluxes, as well as those of N_2O from Guimarães and de Mello (2008), we obtained average emissions of 92.2 g CO_2-eq m^{-2} yr^{-1} for CH_4 and 20.9 g CO_2-eq m^{-2} yr^{-1} for N_2O. These numbers can be compared with the average CO_2 uptake by the bay of 531.8 g CO_2-eq m^{-2} yr^{-1}. As a result, the negative radiative balance of Guanabara Bay due to the CO_2 uptake is lowered by the CH_4 and N_2O emissions by 17% and 4%, respectively. Therefore, eutrophication amplifies the CO_2 sink. However, it is counteracted by the emissions of CH_4 and N_2O in the polluted sectors of Guanabara Bay.

Conclusions

Our results show that Guanabara Bay presented a large spatial and temporal variability in CH_4 concentrations and emissions. Temporally, highest CH_4 concentrations and emissions were detected in the wet period, following strong precipitation events that can enhance the wash-out and flush the urban areas, sewage network and polluted rivers. Spatially, the most polluted sector at the vicinity of the major sewage outlet presented the highest CH_4 concentrations. This polluted sector represents only about 10% of the total surface area of the Bay, but is responsible for half of the total diffusive CH_4 flux. CH_4 did not correlate with the other physico-chemical aquatic parameters analysed in this study, and did not show differences between bottom and surface waters, even when stratification of the water column and vertical gradients of other biogeochemical parameters occurred. These characteristics, as well as the modest sedimentation rates in the Bay, lead to the hypothesis that the CH_4 is mostly allochtonous and that, because of the high salinity and availability of sulphate, methanogenesis is not important in the sediments at centre of the bay itself to generate significant amounts of CH_4.

The concentrations and emissions of CH_4 in Guanabara Bay are among the highest reported in estuarine emitters worldwide. Taking into account that the eutrophication and pollution in coastal waters will increase especially in tropical regions as the result of anthropogenic pressure (the tropical regions include countries with the largest population growth), the CH_4 emissions also tend to be enhanced in highly disturbed ecosystems. According to the compiled CH_4 fluxes, urban pollution appears as one significant source of CH_4 to the estuaries and coastal waters. Henceforth, comparative studies of human-disturbed and pristine estuaries in the tropics and subtropics should be conducted to improve our understanding of coastal carbon dynamics and greenhouse emissions in the tropics and better estimating the global CH_4 estuarine flux. This global flux is indeed based on data collected mainly in temperate and boreal regions.

The eutrophication in Guanabara Bay tends to promote CO_2 uptake (Cotovicz et al. 2015), whereas for CH_4 the strong organic pollution tends to favour emissions to the atmosphere. Comparing the fluxes of CO_2 (Cotovicz et al. 2015) with the CO_2-eq emissions for CH_4 (this study) and N_2O (Guimarães and de Mello 2008), the sink character for CO_2 is counterweighted by the emissions character for CH_4 and N_2O. It entails that the negative radiative balance of Guanabara Bay due to CO_2 uptake is lowered by the CH_4 and N_2O emissions at about 20%. Amplification of the number and more efficient urban wastewater treatments must be encouraged due to the multiple benefits for the mitigation of greenhouse gas emissions, thus improving public health, conservation of water resources and reduction of untreated discharges to water and soils (IPCC 2013).

References

Abril, G., and N. Iversen. 2002. Methane dynamics in a shallow, non-tidal, estuary (Randers Fjord, Denmark). Mar. Ecol. Prog. Ser. **230**: 171–181. doi:10.3354/meps230171

Abril, G., M. V. Commarieu, and F. Guérin. 2007. Enhanced methane oxidation in an estuarine turbidity maximum. Limnol. Oceanogr. **52**: 470–475. doi:10.4319/lo.2007.52.1.0470

Abril, G., M. V. Commarieu, A. Sottolichio, P. Bretel, and F. Guérin. 2009. Turbidity limits gas exchange in a large macrotidal estuary. Estuar. Coast. Shelf Sci. **83**: 342–348. doi:10.1016/j.ecss.2009.03.006

Allen, D., R. C. Dalal, H. Rennenberg, and S. Schmidt. 2010. Seasonal variation in nitrous oxide and methane emissions from subtropical estuary and coastal mangrove sediments, Australia. Plant Biol. **13**: 126–133. doi:10.1111/j.1438-8677.2010.00331.x

Bange, H. W. 2006. Nitrous oxide and methane in European coastal waters. Estuar. Coast. Shelf Sci. **70**: 361–374. doi:10.1016/j.ecss.2006.05.042

Barnes, J., and others. 2006. Tidal dynamics and rainfall control N_2O and CH_4 emissions from a pristine mangrove creek. Geophys. Res. Lett. **33**: L15405. doi:10.1029/2006GL026829

Bartlett, K. B., D. S. Bartlett, R. C. Harris, and D. I. Sebacher. 1987. Methane emissions along a salt marsh salinity gradient. Biogeochemistry **4**: 183–202. doi:10.1007/BF02187365

Bérgamo, A. S. 2006. Características hidrográficas, da circulação, e dos transportes de volume e sal na Baia de Guanabara (RJ): variações sazonais e moduladas pela mare. Ph.D. thesis. Universidade de São Paulo.

Bidone, E. D., and L. D. Lacerda. 2004. The use of DPSIR framework to evaluate sustainability in coastal areas, case study: Guanabara Bay Basin, Rio de Janeiro, Brazil. Reg. Environ. Change **4**: 5–16. doi:10.1007/s10113-003-0059-2

Biswas, H., S. K. Mukhopadhyay, S. Sen, and T. K. Jana. 2007. Spatial and temporal patterns of methane dynamics

in the tropical mangrove dominated estuary, NE coast of Bay of Bengal, India. J. Mar. Syst. **68**: 55–64. doi:10.1016/j.jmarsys.2006.11.001

Blair, N. E., and R. C. Aller. 1995. Anaerobic methane oxidation on the Amazon shelf. Geochim. Cosmochim. Acta **59**: 3707–3715. doi:10.1016/0016-7037(95)00277-7

Borges, A. C., C. J. Sanders, H. L. R. Santos, D. R. Araripe, W. Machado, and S. R. Patchineelam. 2009. Eutrophication history of Guanabara Bay (SE Brazil) recorded by phosphorus flux to sediments from a degraded mangrove area. Mar. Pollut. Bull. **58**: 1750–1754. doi:10.1016/j.marpolbul.2009.07.025

Borges, A. V., and G. Abril. 2011. Carbon dioxide and methane dynamics in estuaries, p. 119–161. *In* W. Eric and M. Donald [eds.], Treatise on estuarine and coastal science. Academic Press.

Bousquet, P., and others. 2006. Contribution of anthropogenic and natural sources to atmospheric methane variability. Nature **443**: 439–443. doi:10.1038/nature05132

Burgos, M., A. Sierra, T. Ortega, and J. M. Forja. 2015. Anthropogenic effects on greenhouse gas (CH4 and N2O) emissions in the Guadalete River Estuary (SW Spain). Sci. Total Environ. **503–504**: 179–189. doi:10.1016/j.scitotenv.2014.06.038

Call, M., and others. 2015. Spatial and temporal variability of carbon dioxide and methane fluxes over semi-diurnal and spring–neap–spring timescales in a mangrove creek. Geochim. Cosmochim. Acta **150**: 211–225. doi:10.1016/j.gca.2014.11.023

Carreira, R. S., A. L. R. Wagener, J. W. Readman, T. W. Fileman, S. A. Macko, and A. Veiga. 2002. Changes in the sedimentary organic carbon pool of a fertilized tropical estuary, Guanabara Bay, Brazil: An elemental, isotopic and molecular marker approach. Mar. Chem. **79**: 207–227. doi:10.1016/S0304-4203(02)00065-8

Castro-Morales, K., J. V. Macías-Zamora, S. R. Canino-Herrera, and R. A. Burke. 2014. Dissolved methane concentration and flux in the coastal zone of the Southern California Bight-Mexican sector: Possible influence of wastewater. Estuar. Coast. Shelf Sci. **144**: 65–74. doi:10.1016/j.ecss.2014.04.017

Chen, C.-T. A., and others. 2008. Hydrogeochemistry and greenhouse gases of the Pearl River, its estuary and beyond. Quat. Int. **186**: 79–90. doi:10.1016/j.quaint.2007.08.024

Cotovicz, L. C., Jr., B. A. Knoppers, N. Brandini, S. J. Costa Santos, and G. Abril. 2015. A strong CO_2 sink enhanced by eutrophication in a tropical coastal embayment (Guanabara Bay, Rio de Janeiro, Brazil). Biogeosciences. **12**: 6125–6146. doi:10.5194/bg-12-6125-2015

de Angelis, M. A., and M. D. Lilley. 1987. Methane in surface waters of Oregon estuaries and rivers. Limnol. Oceanogr. **32**: 716–722. doi:10.4319/lo.1987.32.3.0716

de Angelis, M. A., and M. I. Scranton. 1993. The fate of methane in the Hudson River and estuary. Global Biogeochem. Cycles **7**: 509–523. doi:10.1029/93GB01636

Dutta, M. K., R. Mukherjee, T. K. Jana, and S. K. Mukhopadhyay. 2015. Biogeochemical dynamics of exogenous methane in an estuary associated to a mangrove biosphere; The Sundarbans, NE coast of India. Mar. Chem. **170**: 1–10. doi:10.1016/j.marchem.2014.12.006

EPA. 2010. Methane and nitrous oxide emissions from natural sources. Report EPA 430-R-10-001. U.S. Environmental Protection Agency.

Fenchel, T., C. Bernard, G. Esteban, B. J. Findlay, P. J. Hansen, and N. Iversen. 1995. Microbial diversity and activity in a Danish fjord with anoxic deep waters. Ophelia **43**: 45–100. doi:10.1080/00785326.1995.10430576

Fistarol, G. O., and others. 2015. Environmental and sanitary conditions of Guanabara Bay, Rio de Janeiro. Front. Microbiol. **6**: 1232. doi:10.3389/fmicb.2015.01232

Godoy, J. M., A. V. Oliveira, A. C. Almeida, M. L. Godoy, I. Moreira, A. R. Wagener, and A. G. Figueiredo Junior. 2012. Guanabara Bay sedimentation rates based on 210Pb dating: Reviewing the existing data and adding new data. J. Braz. Chem. Soc. **23**: 1265–1273. doi:10.1590/S0103-50532012000700010

Grasshoff, K., M. Ehrhardt, and K. Kremling. 1999. Methods of seawater analysis, 3rd ed. Wiley-VCH.

Guérin, F., and others. 2007. Gas transfer velocities of CO_2 and CH_4 in a tropical reservoir and its river downstream. J. Mar. Syst. **66**: 161–172. doi:10.1016/j.jmarsys.2006.03.019

Guimarães, G. P., and W. Z. de Mello. 2008. Fluxos de óxido nitroso na interface ar-mar na Baía de Guanabara. Quim. Nova **31**: 1613–1620. doi:10.1590/S0100-40422008000700003

IPCC. 2013. Climate Change 2013: The Physical Science Basis. Contribution of Working Group I to the Fifth Assessment Report of the Intergovernmental Panel on Climate Change. *In* T. F. Stocker, and others [eds.], Cambridge Univ. Press. doi:10.1017/CBO9781107415324

Jähne, B., K. O. Munnich, R. Bosinger, A. Dutzi, W. Huber, and P. Libner. 1987. On parameters influencing air-water exchange. J. Geophys. Res. **92**: 1937–1949. doi:10.1029/JC092iC02p01937

Kelley, C. A., C. S. Martens, and J. P. Chanton. 1990. Variations in sedimentary carbon remineralization rates in the White Oak River estuary, North Carolina. Limnol. Oceanogr. **35**: 372–383. doi:10.4319/lo.1990.35.2.0372

Kjerfve, B., C. A. Ribeiro, G. T. M. Dias, A. Filippo, and V. S. Quaresma. 1997. Oceanographic characteristics of an impacted coastal bay: Baia de Guanabara, Rio de Janeiro, Brazil. Cont. Shelf Res. **17**: 1609–1643. doi:10.1016/S0278-4343(97)00028-9

Koné, Y. J. M., G. Abril, B. Delille, and A. V. Borges. 2010. Seasonal variability of methane in the rivers and lagoons of Ivory Coast (West Africa). Biogeochemistry **100**: 21–37. doi:10.1007/s10533-009-9402-0

Kristensen, E., M. R. Flindt, S. Ulomi, A. V. Borges, G. Abril, and S. Bouillon. 2008. Emission of CO_2 and CH_4 to the

atmosphere by sediments and open waters in two Tanzanian mangrove forests. Mar. Ecol. Prog. Ser. **370**: 53–67. doi:10.3354/meps07642

Maher, D. T., K. Cowley, I. R. Santos, P. Macklin, and B. D. Eyre. 2015. Methane and carbon dioxide dynamics in a subtropical estuary over a diel cycle: Insights from automated in situ radioactive and stable isotope measurements. Mar. Chem. **168**: 69–79. doi:10.1016/j.marchem.2014.10.017

Martens, C. S., and R. A. Berner. 1974. Methane production in sulphate-depleted marine sediments. Science **18**: 1167–l169. doi:10.1126/science.185.4157.1167

Martens, C. S., and R. A. Berner. 1977. Interstitial water chemistry of anoxic Long Island Sound sediments. 1. Dissolved gases. Limnol. Oceanogr. **22**: 10–25. doi:10.4319/lo.1977.22.1.0010

Martens, C. S., and J. V. Klump. 1980. Biogeochemical cycling in an organic-rich coastal marine basin—I. Methane sediment–water exchange processes. Geochim. Cosmochim. Acta **44**: 471–490. doi:10.1016/0016-7037(80)90045-9

Martens, C. S., D. B. Albert, and M. J. Alperin. 1998. Biogeochemical processes controlling methane in gassy coastal sediments—part 1. A model coupling organic matter flux to gas production, oxidation and transport. Cont. Shelf Res. **18**: 1741–1770. doi:10.1016/S0278-4343(98)00056-9

Middelburg, J. J., G. Klaver, J. Nieuwenhuize, A. Wielemaker, W. Haas,T. Vlut, F. J. W. A. Van der Nat. 1996. Organic matter mineralization in intertidal sediments along an estuarine gradient. Mar. Ecol. Prog. Ser. **132**: 157–168. doi:10.3354/meps132157.

Middelburg, J. J., J. Nieuwenhuize, N. Iversen, N. Høgh, H. de Wilde, W. Helder, R. Seifert, and O. Christof. 2002. Methane distribution in tidal estuaries. Biogeochemistry **59**: 95–119. doi:10.1023/A:1015515130419

Nirmal Rajkumar, A., J. Barnes, R. Ramesh, R. Purvaja, and R. C. Upstill-Goddard. 2008. Methane and nitrous oxide fluxes in the polluted Adyar River and estuary, SE India. Mar. Pollut. Bull. **56**: 2043–2051. doi:10.1016/j.marpolbul.2008.08.005

Paranhos, R., A. P. Pereira, and L. M. Mayr. 1998. Diel variability of water quality in a tropical polluted bay. Environ. Monit. Assess. **50**: 131–141. doi:10.1023/A:1005855914215

Ramesh, R., R. Purvaja, V. Neetha, J. Divia, J. Barnes, and R. C. Upstill-Goddard. 2007. CO_2 and CH_4 emissions from Indian mangroves and its surrounding waters. *In* Y. Tateda, R. C. Upstill-Goddard, T. Goreau, D. Alongi, E. Kristensen, and G. Wattayakorn [eds.], Greenhouse gas and carbon balances in mangrove coastal ecosystems. Gendai Tosho, Kanagawa.

Raymond, P. A., and J. J. Cole. 2001. Gas exchange in rivers and estuaries: Choosing a gas transfer velocity. Estuaries **24**: 312–317. doi:10.2307/1352954

Reeburgh, W. S. 2007. Oceanic methane biogeochemistry. Chem. Rev. **107**: 486–513. doi:10.1021/cr050362v

Ribeiro, C. H. A., and B. Kjerfve. 2002. Anthropogenic influence on the water quality in Guanabara Bay, Rio de Janeiro, Brazil. Reg. Environ. Change **3**: 13–19. doi:10.1007/s10113-001-0037-5

Sansone, F. J., M. E. Holmes, and B. N. Popp. 1999. Methane stable isotopic ratios and concentrations as indicators of methane dynamics in estuaries. Global Biogeochem. Cycles **13**: 463–474. doi:10.1029/1999GB900012

Strickland, J. D. H., and T. R. Parsons. 1972. A practical handbook of seawater analysis, 2nd ed. Fisheries Research Board of Canada Bulletin.

Turque, A. S., and others. 2010. Environmental shaping of sponge associated archaeal communities. PLoS One **5**: e15774. doi:10.1371/journal.pone.0015774

Upstill-Goddard, R. C., J. Barnes, T. Frost, S. Punshon, and N. J. P. Owens. 2000. Methane in the Southern North Sea: Low salinity inputs, estuarine removal and atmospheric flux. Global Biogeochem. Cycles **14**: 1205–1217. doi:10.1029/1999GB001236

Vieira, R. P., and others. 2007. Archaeal communities in a tropical estuarine ecosystem: Guanabara Bay, Brazil. Microb. Ecol. **54**: 460–462. doi:10.1007/s00248-007-9261-y

Wanninkhof, R. 1992. Relationship between gas exchange and wind speed over the ocean. J. Geophys. Res. **97**: 7373–7382. doi:10.1029/92JC00188

Yamamoto, S., J. B. Alcauskas, and T. E. Crozier. 1976. Solubility of methane in distilled water and seawater. J. Chem. Eng. Data **21**: 78–80. doi:10.1021/je60068a029

Zhang, G., J. Zhang, S. Lui, J. Ren, J. Xu, and F. Zhang. 2008. Methane in the Changjiang (Yangtze River) Estuary and its adjacent marine area: Riverine input, sediment release and atmospheric fluxes. Biogeochemistry **91**: 71–84. doi:10.1007/s10533-008-9259-7

Zhou, H., X. Yin, Q. Yang, H. Wang, Z. Wu, and S. Bao. 2009. Distribution, source and flux of methane in the western Pearl River Estuary and northern South China Sea. Mar. Chem. **117**: 21–31. doi:10.1016/j.marchem. 2009.07.011

Acknowledgments

We are grateful to Ludmila P. Costa and Renato C. Cordeiro (FAPERJ Project Proc. Nr. E-26/111.190/2011) for their logistical support. We would like to thank the three anonymous reviewers for their valuable comments and suggestions. This research was funded by the Science without Border Program of the Brazilian National Council of Research and Development (CNPq-PVE Proc. Nr 401726-6), including a Senior Scientist grant to G. Abril, a Post-Doc grant to N. Brandini and a Ph.D. grant to L.C. Cotovicz Jr for his internship at EPOC, Université Bordeaux. B. Knoppers is a Senior Scientist of CNPq (Proc. Nr. 301572/2010-0). The global estuarine data were kindly provided by Alberto Borges (Université de Liége).

Submitted 4 September 2015
Revised 27 January 2016
Accepted 29 February 2016

Associate editor: Leila Hamdan